CMS Physics Analysis Summary

Contact: cms-pag-conveners-higgs@cern.ch 2011/07/22

Search for Neutral Higgs Bosons Decaying to Tau Pairs in pp Collisions at $\sqrt{s} = 7$ TeV

The CMS Collaboration

Abstract

A search for neutral Higgs bosons in proton-proton collisions at the LHC at a center-of-mass energy of 7 TeV is presented. The results are based on a data sample corresponding to an integrated luminosity of 1.1/fb recorded by the CMS experiment. The search uses decays of the Higgs bosons to tau pairs, including the cases where the Higgs boson is produced in association with a b-quark jet (MSSM search) or two forward jets from vector boson fusion Higgs boson production (SM search). No excess is observed in the tau-pair invariant-mass spectrum. The resulting upper limits on the Higgs boson production cross section times branching fraction to tau pairs, as a function of the pseudoscalar Higgs boson mass, yield stringent new bounds in the MSSM parameter space.

1 Introduction

The standard model (SM) has been extremely successful in describing a wide range of phenomena in particle physics, and has survived some four decades of experimental testing. The search is underway at the Large Hadron Collider (LHC) for the only remaining undiscovered particle predicted by the SM, the Higgs boson [1–5]. A promising experimental channel for this search is the production of Higgs bosons via vector boson fusion (VBF), with subsequent decay of the Higgs bosons to τ pairs.

However, the Higgs boson in the SM suffers from quadratically divergent self-energy corrections at high energies [6]. Numerous extensions to the SM have been proposed to address these divergences. One such model, supersymmetry [7], a symmetry between fundamental bosons and fermions, results in cancellation of the divergences. The minimal supersymmetric extension to the standard model (MSSM) requires the presence of two Higgs doublets. This leads to a more complicated scalar sector, with five massive Higgs bosons: a light neutral CP-even state (h), two charged states ($H^{\pm}$), a heavy neutral CP-even state (H) and a neutral CP-odd state (A).

The mass relations among the neutral MSSM Higgs bosons are such that if $m_A \lesssim 130$ GeV, at large values of the parameter $\tan\beta$ the masses of the h and A are nearly degenerate, while that of the H is approximately 130 GeV. If $m_A \gtrsim 130$ GeV, then the masses of the A and H are nearly degenerate, while that of the h remains near 130 GeV. The precise value of the crossover point depends predominantly on the nature of the mass mixing in the top-squark states.

This Summary reports a search for the SM and the neutral MSSM Higgs bosons in pp collisions at $\sqrt{s} = 7$ TeV at the LHC, using a data sample collected in 2011 corresponding to 1.1 fb^{-1} of integrated luminosity recorded by the Compact Muon Solenoid (CMS) experiment. This search, an extension to our previous search for neutral Higgs bosons decaying to τ pairs [8], is similar to those performed at the Tevatron [9] and by the ATLAS experiment [10] and is complementary to the MSSM Higgs search at LEP [11].

In the case of SM Higgs bosons, the gluon-fusion production of Higgs bosons has the largest cross section, but the background from QCD production of $\mathrm{b\bar{b}}$ and Drell-Yan production of tau pairs in the mass region of interest overwhelm the expected Higgs boson signal in both the $\mathrm{b\bar{b}}$ and $\tau\tau$ final states. To overcome this we rely on the VBF production of Higgs bosons, with decays of the Higgs boson to tau pairs, which has better sensitivity. The two forward "tagging" jets from the incoming quarks which radiate the vector bosons provide means for distinguishing the Higgs boson production from SM background processes.

In the MSSM case, two main production processes contribute to $\mathrm{pp} \to \phi + X$, where $\phi = h, H$, or A: gluon fusion through a b quark loop and direct $\mathrm{b\bar{b}}$ annihilation from the b parton density in the beam protons. In the latter case, there is a significant probability that a b quark jet is produced centrally in association with the Higgs boson.

Four τ pair final states where one or both taus decay leptonically are studied: $\mathrm{e}\tau_h$, $\mu\tau_h$, $\mathrm{e}\mu$, and $\mu\mu$, where we use the symbol τ_h to indicate a reconstructed hadronic decay of a τ.

2 CMS Detector

The central feature of the CMS apparatus is a superconducting solenoid, of 6 m internal diameter, providing a field of 3.8 T. Within the field volume are the silicon pixel and strip tracker, the crystal electromagnetic calorimeter and the brass/scintillator hadron calorimeter. Muons are measured in gas-ionization detectors embedded in the steel return yoke. In addition to the bar-

rel and endcap detectors, CMS has extensive forward calorimetry. Details of the CMS detector and its performance can be found elsewhere [12].

3 Trigger and Event Selection

The triggers used to select the events for this analysis are based on the presence of electron and/or muon trigger objects [13, 14]. With increasing instantaneous luminosity, in order to keep the online transverse momentum thresholds on electrons and muons lower than those used in offline selections, special triggers requiring the presence of both a lepton and an isolated jet consistent with a τ decaying hadronically were adopted for the eτ_h and $\mu\tau_h$ channels.

The analysis presented here makes use of particle flow techniques which combine the information from all CMS sub-detectors to identify and reconstruct individual particles in the event, namely muons, electrons, photons, and charged and neutral hadrons. The detailed description of the algorithm and its commissioning can be found elsewhere [15, 16]. The particle list is given as input to the jet, tau, and missing transverse energy ("$\not\!\!E_{\mathrm{T}}$ ") reconstruction. Hadronically decaying taus are reconstructed using the HPS algorithm described elsewhere [17]. For the $\mu\tau_h$ and eτ_h final states, we select events with an isolated muon with $p_{\mathrm{T}} > 15$ GeV or electron with $p_{\mathrm{T}} > 20$ GeV and $|\eta| < 2.1$, and an oppositely charged τ_h with $p_{\mathrm{T}} > 20$ GeV and $|\eta| < 2.3$.

For the eμ final state, we select events with an isolated electron with $|\eta| < 2.5$ and an oppositely charged isolated muon with $|\eta| < 2.1$, both with $p_{\mathrm{T}} > 15$ GeV. We reject events in which there are more than one e or μ. After the above requirements, the trigger requirements have an efficiency of roughly 90% in the three search channels for $\mathrm{Z} \to \tau\tau$ events.

For the $\mu\mu$ final state, we require two oppositely charged muons with $p_{\mathrm{T}} > 20$ GeV and $|\eta| < 2.1$ for the leading muon and $p_{\mathrm{T}} > 10$ GeV and $|\eta| < 2.4$ for the next-to-leading muon, and emanating from within 0.04 cm of the primary vertex in the transverse plane. The requirement $\not\!\!E_{\mathrm{T}} < 100$ GeV suppresses $\mathrm{t\bar{t}}$ and W+jets background while retaining good signal efficiency. A likelihood ratio discriminant formed from the muon momenta, the $\not\!\!E_{\mathrm{T}}$ and the distance of closest approach of the two muon tracks then helps distinguish the Higgs boson signal from the dominant backgrounds, $\mathrm{Z} \to \mu\mu$ and $\mathrm{Z} \to \tau\tau$.

In tau decays, due to the small invariant mass of the tau lepton, the neutrinos tend to be produced near the visible products. For W+jets decays, one of the main expected backgrounds, due the high mass of the W the neutrino should be approximately opposite the lepton and the jet misidentified as a tau, in the transverse plane. To reject W+jets events we use a discriminator, originally developed by the CDF experiment, formed by considering the bisector of the directions of the visible tau decay products transverse to the beam direction, denoted the ζ axis [18, 19]. From the projection of the visible decay product momenta and the $\not\!\!E_{\mathrm{T}}$ vector onto the ζ axis, two values are calculated:

$$P_\zeta = p_{T,1} \cdot \zeta + p_{T,2} \cdot \zeta + \not\!\!E_{\mathrm{T}}\, \zeta, \tag{1}$$

$$P_\zeta^{\mathrm{vis}} = p_{T,1} \cdot \zeta + p_{T,2} \cdot \zeta \tag{2}$$

For the eτ_h and $\mu\tau_h$ channels, we define the discriminator as

$$P_\zeta^{\mathrm{cut},\ell\tau} = P_\zeta - 1.5 P_\zeta^{\mathrm{vis}}, \tag{3}$$

and we require $P_\zeta^{\mathrm{cut},\ell\tau} > -20$ GeV. For the eμ channel the discriminator is defined as

$$P_\zeta^{\mathrm{cut,e}\mu} = P_\zeta - 1.85 P_\zeta^{\mathrm{vis}}, \tag{4}$$

and we require $P_\zeta^{\mathrm{cut,e}\mu} > -25$ GeV.

The observed number of events in each channel appears in Tables 1 through 4 together with the estimated uncertainty on the yields. The uncertainty on the luminosity is not included for backgrounds estimated using Monte Carlo. The largest source of events selected with these requirements comes from $Z \to \tau\tau$ in all channels except $\mu\mu$. We estimate the contribution from this process using a detailed GEANT4 simulation of the CMS detector, with the events modeled by the MADGRAPH Monte Carlo generator [20]. We determine the normalization for this process based on the number of observed $Z \to ee$ and $Z \to \mu\mu$ events [21]. A significant source of background arises from QCD multijet events and W+jets events in which a jet is misidentified as τ_h, and there is a real or misidentified e or μ. The rates for these processes are estimated using the number of observed same-charge events. Other background processes include $t\bar{t}$ production and $Z \to ee/\mu\mu$ events, particularly in the eτ_h channel, due to the 2–3% probability for electrons to be misidentified as τ_h [17]. The small fake-lepton background from W+jets and QCD for the eμ channel is estimated using data. The dominant background in the $\mu\mu$ channel, $Z \to \mu\mu$, is very challenging and estimated from data.

The event generator PYTHIA and POWHEG are used to model the Higgs boson signal and other backgrounds. The TAUOLA [22] package is used for tau decays in all cases.

		Standard Model		MSSM	
Process	Incl. Sel.	*No VBF*	*VBF*	*No B-Tag*	*B-Tag*
Di-Boson	26.8 ± 8.3	25.5 ± 7.9	0.07 ± 0.05	21.0 ± 6.5	0.39 ± 0.15
$t\bar{t}$	140 ± 16.8	72.0 ± 9.3	0.24 ± 0.12	7.0 ± 1.3	12.5 ± 2.2
Z^{l+jet}	367 ± 45	366 ± 47	0.13 ± 0.05	345 ± 42	2.3 ± 0.3
Z^{ll}	1310 ± 111	1308 ± 122	0.46 ± 0.17	1259 ± 107	8.3 ± 0.7
$W + jets$	1669 ± 118	1646 ± 114	0.58 ± 0.22	1524 ± 106	10.6 ± 0.8
QCD	3222 ± 179	3198 ± 177	3.2 ± 2.4	3079 ± 169	49.8 ± 8.7
$Z \to \tau\tau$	3400 ± 239	3366 ± 272	1.2 ± 0.4	3163 ± 222	21.5 ± 1.6
Total Background	10136 ± 343	9980 ± 302	5.9 ± 2.5	9398 ± 320	105 ± 9.2
Data	10960	10787	7	10283	101
Signal Efficiency					
$bb \to \phi$	0.014	-	-	0.012	0.0040
$gg \to \phi$	0.013	-	-	0.013	0.00023
$gg \to H$	0.014	0.013	4.5×10^{-5}	-	-
$qq \to qqH$	0.014	0.012	0.0015	-	-

Table 1: Number of expected and observed events after the inclusive selection and in the event categories as described the text for the eτ_h channel. Also given are the signal acceptances for a MSSM Higgs boson with $m_A = 120$ GeV via gluon-gluon fusion and $b\bar{b}$ annihilation and for a SM Higgs boson with $m_H = 120$ GeV produced via gluon-gluon fusion and VBF. All acceptances include the branching ratio into $\tau\tau$.

To further explore the characteristics of the production of Higgs bosons both in the SM and in the MSSM we split the sample of selected events in several categories based on the number of selected jets and b-tagged jets. In the SM case, we select events with the jet signature of VBF, which is two jets with a wide separation in pseudorapidity. In the MSSM case, there is a significant probability for having a b-tagged jet in the central region, using the "track counting high efficiency" (TCHE) algorithm [23]. We then fit the observed mass distributions in each case to the sum of the standard model backgrounds and the Higgs boson signal.

		Standard Model		MSSM	
Process	Incl. Sel.	*No VBF*	*VBF*	*No B-Tag*	*B-Tag*
Di-Boson	64.7 ± 19.8	62.2 ± 19.0	0.16 ± 0.08	53.8 ± 16.5	1.01 ± 0.34
$t\bar{t}$	312 ± 36.7	166 ± 19.7	1.07 ± 0.29	15.7 ± 2.73	29.4 ± 4.92
Z^{l+jet}	233 ± 30.2	231 ± 30.0	0.08 ± 0.03	221 ± 30.9	1.47 ± 0.19
Z^{ll}	131 ± 34.4	131 ± 34.3	0.05 ± 0.02	124 ± 33.3	0.83 ± 0.22
$W + jets$	2813 ± 191	2815 ± 185	0.98 ± 0.37	2669 ± 173	17.8 ± 1.28
QCD	2663 ± 122	2608 ± 119	8.48 ± 3.73	2454 ± 111	81.6 ± 10.6
$Z \to \tau\tau$	9619 ± 653	9531 ± 647	3.37 ± 1.25	8977 ± 610	60.8 ± 4.4
Total Background	15836 ± 693	15544 ± 685	14.2 ± 3.95	14514 ± 640	193 ± 13
Data	16308	15988	18	15057	243
Signal Efficiency					
$bb \to \phi$	0.027	-	-	0.0240	0.00673
$gg \to \phi$	0.025	-	-	0.0242	0.00045
$gg \to H$	0.025	0.024	0.0001	-	-
$qq \to qqH$	0.027	0.023	0.0027	-	-

Table 2: Number of expected and observed events after the Inclusive Selection and in the event categories as described the text for the $\mu\tau_h$ channel. Also given are the signal acceptances for a MSSM Higgs boson with $m_A = 120$ GeV via gluon-gluon fusion and $b\bar{b}$ annihilation and for a SM Higgs boson with $m_H = 120$ GeV produced via gluon-gluon fusion and VBF. All acceptances include the branching ratio into $\tau\tau$.

		Standard Model		MSSM	
Process	Incl. Sel.	*Non VBF*	*VBF*	*Non B-Tag*	*B-Tag*
Di-Boson	164 ± 49	154 ± 46	1.0 ± 0.3	117 ± 35	16 ± 5
$t\bar{t}$	637 ± 64	400 ± 40	3.0 ± 0.3	51 ± 5	80 ± 8
Fakes	334 ± 100	318 ± 95	0.0 ± 0.0	272 ± 82	16 ± 8
$Z \to \tau\tau$	3411 ± 102	3379 ± 101	2.8 ± 0.8	3203 ± 96	38 ± 1.9
Total Background	4546 ± 164	4251 ± 151	6.7 ± 0.9	3643 ± 131	150 ± 12
Data	4772	4517	2	3942	143
Signal Efficiency					
$gg \to \phi$	0.00854	-	-	0.00769	0.00010
$bb \to \phi$	0.00845	-	-	0.00859	0.00115
$qq \to H$	0.00781	0.00755	0.00007	-	-
$qq \to qqH$	0.00971	0.00837	0.00134	-	-

Table 3: Number of expected and observed events after the lepton selection, the inclusive selection and in the event categories as described the text for the eμ channel. Also given are the signal acceptances for a MSSM Higgs boson with $m_A = 120$ GeV via gluon-gluon fusion and $b\bar{b}$ annihilation and for a SM Higgs boson with $m_H = 120$ GeV produced via gluon-gluon fusion and VBF. The acceptances include the branching ratio into $\tau\tau$.

- ***SM*** The SM fit has two categories, which are mutually exclusive:
  - ***VBF*** Requires exactly 2 jets with $p_T > 30$ GeV, $M_{jj} > 350$ GeV, $|\Delta\eta_{jj}| > 3.5$ and $\eta_1 \cdot \eta_2 < 0$.
  - ***Non-VBF*** Requires less or equal to 1 jet with $p_T > 30$ GeV, or exactly two jets which fail at least one of the above requirements.
- ***MSSM*** The MSSM fit also has two categories, which are mutually exclusive:
  - ***b-Tag*** At most 1 jet with $p_T > 30$ GeV, at least one b-tagged jet with $p_T > 20$ GeV.

		Standard Model		MSSM	
Process	Incl. Sel.	*Non VBF*	*VBF*	*Non B-Tag*	*B-Tag*
$Z/\gamma^* \to \mu\mu$	17255 ± 117	16862 ± 115	87.7 ± 7.0	15219 ± 105	428 ± 11
$Z/\gamma^* \to \tau\tau$	427 ± 8.8	420 ± 17	1.79 ± 0.47	404 ± 8.3	3.51 ± 0.74
$t\bar{t}$	146 ± 18	101 ± 12	2.11 ± 0.27	14.2 ± 2.2	28.4 ± 4.4
QCD	6.2 ± 1.1	5.7 ± 1.0	–	5.7 ± 1.0	0.55 ± 0.55
$W + jets$	3.7 ± 2.0	3.7 ± 2.0	–	2.8 ± 1.6	–
Total	17837 ± 118	17392 ± 117	91.6 ± 7.0	15645 ± 105	460 ± 12
Data	17925	17596	103	15711	479
Signal Efficiency (SM/MSSM)					
$gg \to \phi$	0.00162	-	-	0.00148	2.77×10^{-5}
$bb \to \phi$	0.00172	-	-	0.00139	2.83×10^{-4}
$gg \to H$	0.00166	0.00164	2.96×10^{-5}	-	-
$qq \to qqH$	0.00180	0.00147	5.56×10^{-4}	-	-

Table 4: Number of expected and observed events after the lepton selection, the inclusive selection and in the event categories as described the text for the $\mu\mu$ channel. Also given are the signal acceptances for a MSSM Higgs boson with $m_A = 120$ GeV via gluon-gluon fusion and $b\bar{b}$ annihilation and for a SM Higgs boson with $m_H = 120$ GeV produced via gluon-gluon fusion and VBF. The acceptances include the branching ratio into $\tau\tau$.

- ***No b-Tag*** At most 1 jet with $p_T > 30$ GeV, no b-tagged jet with $p_T > 20$ GeV.

4 Systematic Uncertainties

Various imperfectly known or imperfectly simulated effects can alter the shape and normalization of the visible mass spectrum. The main sources of normalization uncertainties include the total integrated luminosity (6%) [24], jet energy scale (5%), background normalization (Table 1-4), Z production cross section (3%) [21], and lepton identification and isolation efficiency (1.0%) and trigger (1.0%). The tau identification efficiency uncertainty is estimated to be 6% from an independent study using a tag and probe technique. In the SM search theoretical uncertainty on the Higgs production are included (12% for ggH and 3.5% for qqH [25]) and in the MSSM search the uncertainty on the efficiency to identify a b-jet (10%) is considered [26]. Uncertainties that contribute to mass spectrum shape variations include the tau (3%), muon (1%), and electron (2%) energy scales.

5 Likelihood Fit

To search for the presence of a Higgs boson signal in the selected events, we perform a maximum likelihood fit to the tau-pair visible-mass spectrum. In the eτ, $\mu\tau$, and eμ channels we use m_{vis}. In the case of the $\mu\mu$ channel the fit is performed in the 2D space of m_{vis} versus m_{fit}, where the latter is the result of a event-by-event likelihood fit for the tau pair invariant mass, imposing all available kinematic constraints [8].

Systematic uncertainties are represented by nuisance parameters, which we remove by marginalization, assuming a log normal prior for normalization parameters, and Gaussian priors for mass-spectrum shape uncertainties. The uncertainties that affect the shape of the mass spectrum, mainly those corresponding to the energy scales, are represented by nuisance parameters whose variation results in a continuous modification of the spectrum shape [27].

The parameter representing the tau identification uncertainty affects taus from the Higgs boson signal and the main background, $Z \to \tau\tau$, equally. This effectively allows the observed $Z \to \tau\tau$ events to provide an *in situ* calibration of this efficiency, except for Higgs boson masses near that of the Z.

Figures 1 – 4 show the distributions of the tau-pair visible mass m_{vis}, defined as the invariant mass of the visible tau decay products, for the four search channels, for each category, compared with the background prediction in each category.

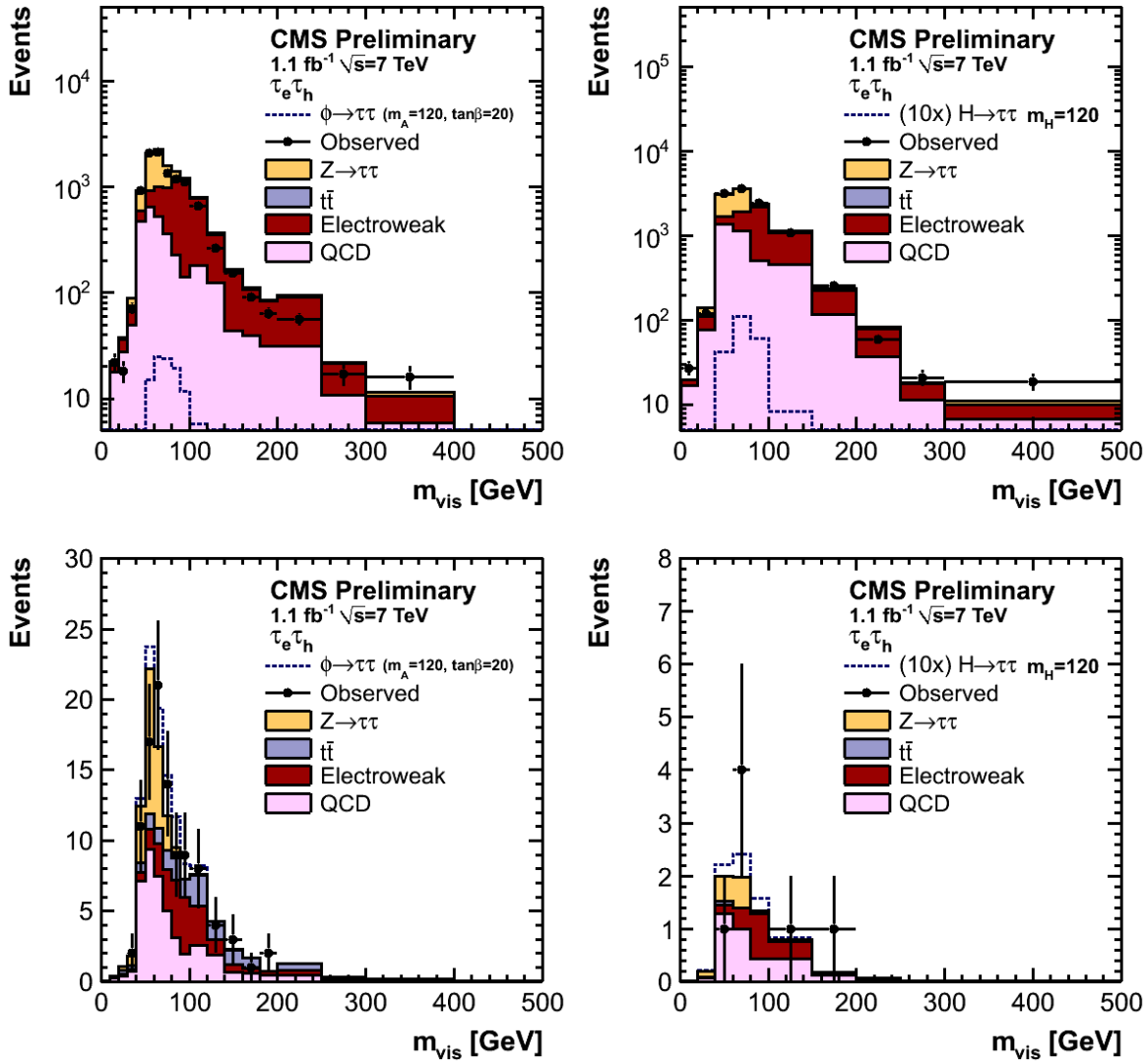

Figure 1: Visible mass, m_{vis} for events in the eτ_h channel, in the No b-Tag category (upper left), Non-VBF (upper right), b-Tag category (lower left) and VBF category (lower right).

6 MSSM Higgs Results

The mass spectra show no evidence for the presence of a Higgs boson signal, and we set 95% CL (confidence level) upper bounds on the Higgs boson cross section times the tau-pair branching fraction (denoted by $\sigma_\phi \cdot B_{\tau\tau}$).

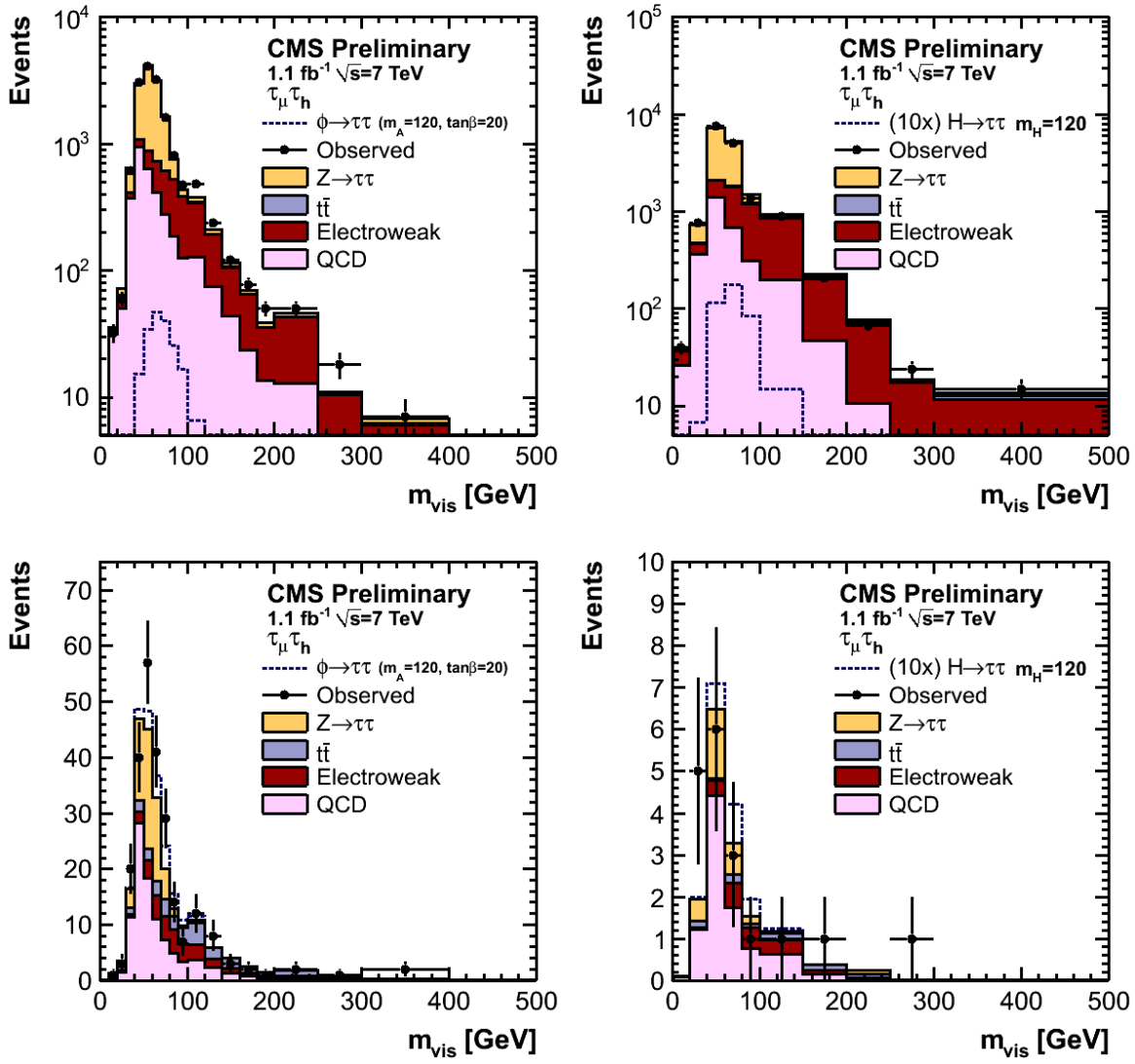

Figure 2: Visible mass, m_{vis} for events in the $\mu\tau_h$ channel, in the No b-Tag category (upper left), Non-VBF (upper right), b-Tag category (lower left) and VBF category (lower right).

Figure 5 shows the upper bound on $\sigma_\phi \cdot B_{\tau\tau}$ as a function of m_A, where we use as the signal acceptance model the combined mass spectra from the gg and $b\bar{b}$ production processes for h, A, and H, and assuming $\tan\beta = 30$ [25]. The plot also shows the one- and two-standard-deviation range of expected upper limits for various potential experimental outcomes. The observed limits are well within the expected range assuming no signal. The observed and expected upper limits are shown in Tab. 5.

We can interpret the upper limits on $\sigma_\phi \cdot B_{\tau\tau}$ in the MSSM parameter space of $\tan\beta$ versus m_A for an example scenario. We use here the m_h^{max} [28, 29] benchmark scenario in which M_{SUSY} = 1 TeV; $X_t = 2M_{\text{SUSY}}$; μ = 200 GeV; $M_{\tilde{g}}$ = 800 GeV; M_2 = 200 GeV; and $A_b = A_t$, where M_{SUSY} denotes the common soft-SUSY-breaking squark mass of the third generation; $X_t = A_t - \mu/\tan\beta$ the stop mixing parameter; A_t and A_b the stop and sbottom trilinear couplings, respectively; μ the Higgsino mass parameter; $M_{\tilde{g}}$ the gluino mass; and M_2 the SU(2)-gaugino mass parameter. The value of M_1 is fixed via the GUT relation $M_1 = (5/3)M_2 \sin\theta_W/\cos\theta_W$. In determining these bounds on $\tan\beta$, shown in Table 5 and in Fig. 6, we have used the central values of the

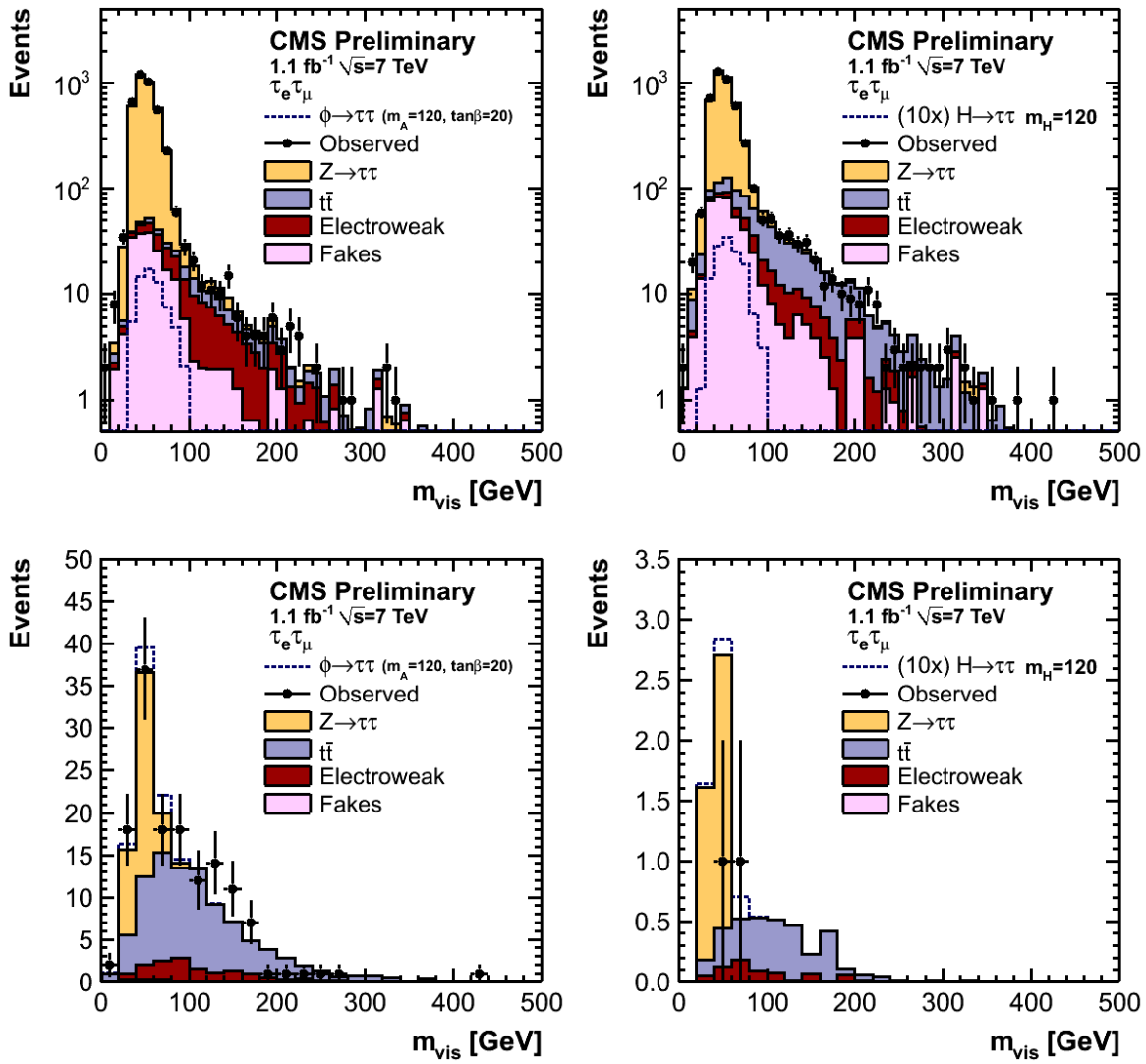

Figure 3: Visible mass, m_{vis} for events in the eμ channel, in the No b-Tag category (upper left), Non-VBF (upper right), b-Tag category (lower left) and VBF category (lower right).

Higgs boson cross sections as a function of $\tan\beta$ reported by the LHC Higgs Cross Section Working Group [25]. The cross sections have been obtained from the GGH@NNLO [30, 31] and HIGLU [32] programs for the gluon-fusion process. For the $b\bar{b} \to \phi$ process, the 4-flavor calculation [33, 34] and the 5-flavor calculation as implemented in the BBH@NNLO [35] program have been combined using the Santander scheme [36]. Rescaling of the corresponding Yukawa couplings by the MSSM factors calculated with FeynHiggs [37] has been applied. We do not quote limits above $\tan\beta = 60$ as the theoretical relation between cross section and $\tan\beta$ becomes unreliable.

The present results exclude a region in $\tan\beta$ down to values smaller than those excluded by the Tevatron experiments [9] for $m_A \lesssim 140$ GeV/c^2, and significantly extend the excluded region of MSSM parameter space at larger values of m_A. Figure 6 also shows the region excluded by the LEP experiments [11].

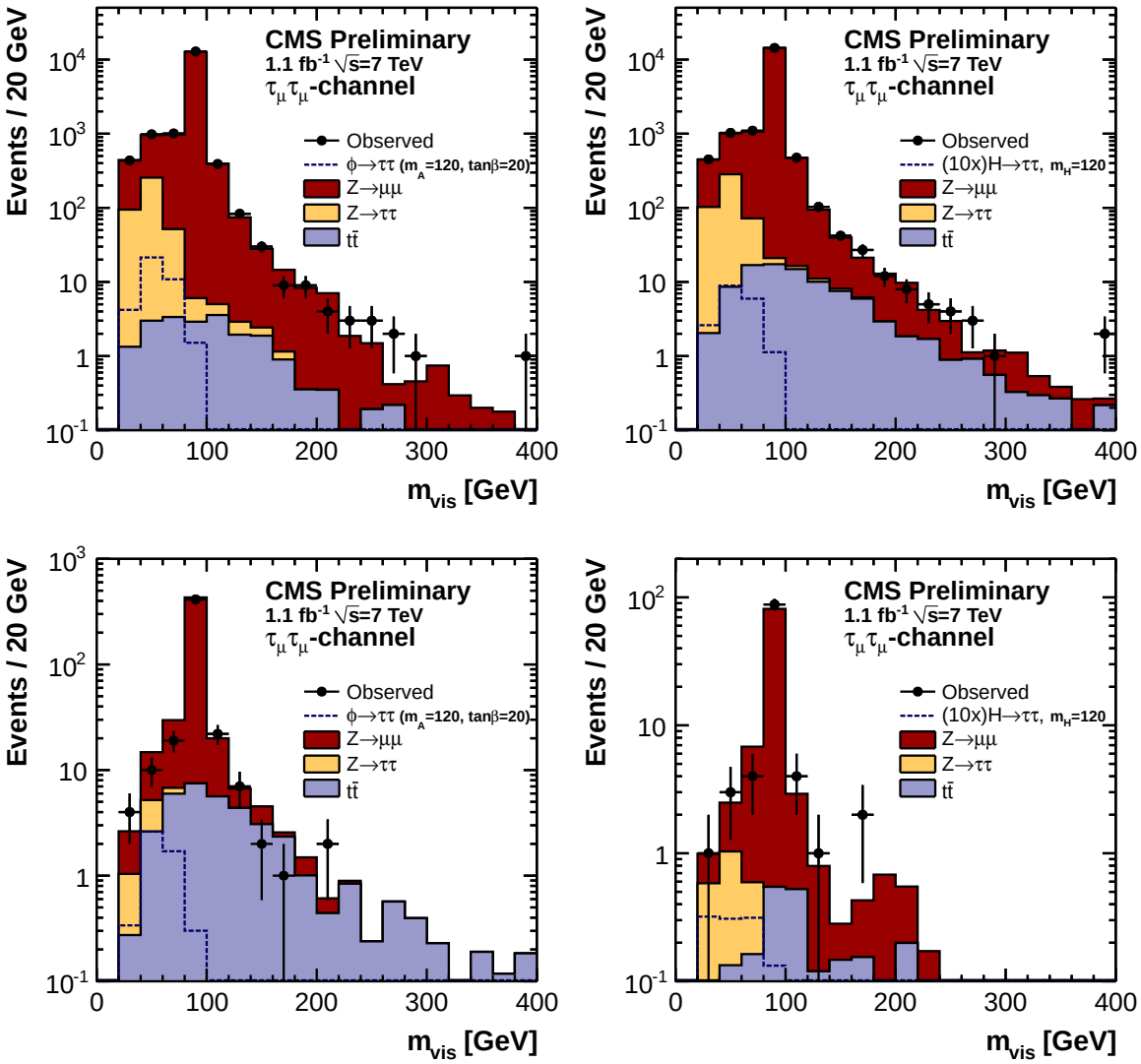

Figure 4: Visible mass, m_{vis} for events in the $\mu\mu$ channel, in the No b-Tag category (upper left), Non-VBF (upper right), b-Tag category (lower left) and VBF category (lower right).

7 SM Higgs Results

In the VBF and Non-VBF categories the mass spectra show no evidence for the presence of a Higgs boson signal. Equivalent to the MSSM search, a maximum likelihood fit to the tau-pair visible-mass spectrum is used to set a 95% CL upper limit on the cross section ratio to the nominal SM Higgs cross section. Figure 7 shows the observed and the mean expected 95% CL upper limits for Higgs mass hypothesis ranging from 110 to 140 GeV/c^2. The bands represent the 1 σ and 2 σ probability intervals around the expected limit. Table 6 shows the result for selected mass values. We set an upper limit on $\sigma_H \cdot B_{\tau\tau}$ of 13-21 times the SM value.

8 Conclusion

In conclusion, we have performed a search for neutral MSSM and SM Higgs bosons, using a sample of CMS data from proton-proton collisions at a center-of-mass energy of 7 TeV at the

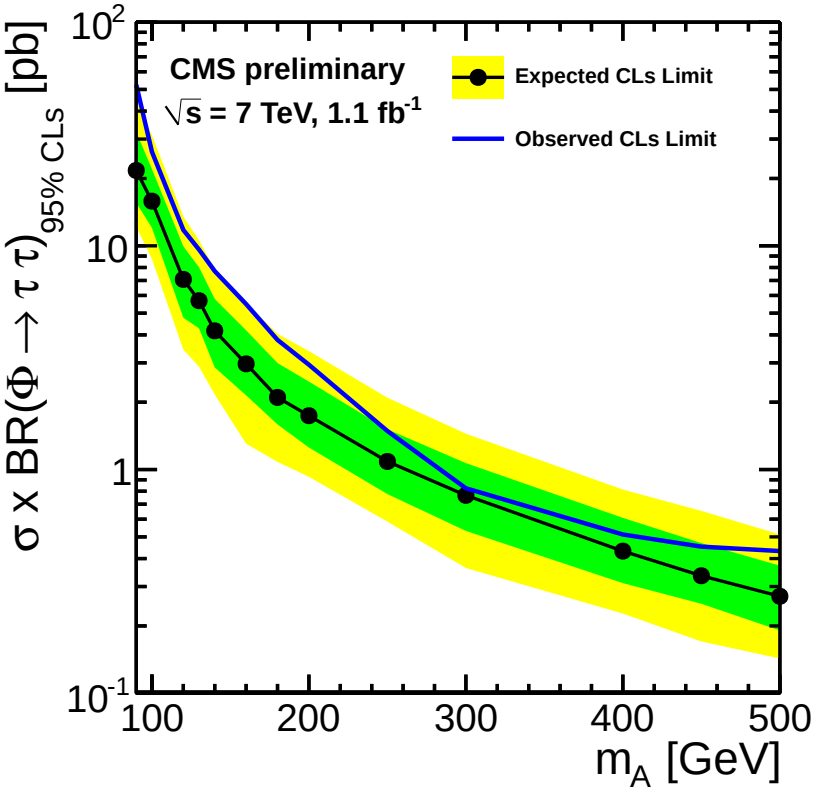

Figure 5: The expected one- and two-standard-deviation ranges and observed 95% CL upper limits on $\sigma_\phi \cdot B_{\tau\tau}$ as a function of m_A. The signal acceptance is based on the MSSM model described in the text, assuming $\tan\beta = 30$.

Table 5: Expected range and observed 95% CL upper limits for $\sigma_\phi \cdot B_{\tau\tau}$ as functions of m_A, for the MSSM search, and 95% CL upper bound on $\tan\beta$ in the $m_h^{\max}$ scenario described in the text. No bounds on $\tan\beta$ above 60 are quoted.

95% CL Upper Limit								
m_A	Expected $\sigma_\phi \cdot B_{\tau\tau}$ (pb)					Observed	Expected	Observed
(GeV)	-2σ	-1σ	Median	$+1\sigma$	$+2\sigma$	(pb)	$\tan\beta$	
90	12.2	15.6	21.7	32.3	44.1	52.5	10.6	16.4
100	8.7	12.0	15.8	22.0	31.2	26.3	11.2	14.3
120	3.4	4.8	7.1	9.9	13.5	11.8	11.0	14.2
130	2.9	4.3	5.7	8.0	10.6	9.6	9.8	13.5
140	2.2	2.9	4.2	5.8	7.9	7.7	11.5	15.7
160	1.3	2.1	3.0	4.2	5.6	5.5	12.4	16.9
180	1.1	1.6	2.1	3.0	4.0	3.8	13.4	17.9
200	0.93	1.3	1.7	2.5	3.4	2.9	15.3	19.7
250	0.56	0.78	1.1	1.5	2.1	1.5	19.7	22.9
300	0.36	0.53	0.77	1.1	1.4	0.83	25.4	26.3
400	0.23	0.31	0.43	0.61	0.81	0.51	38.6	41.7
450	0.17	0.25	0.34	0.47	0.65	0.45	46.0	52.6
500	0.14	0.19	0.27	0.37	0.51	0.43	54.2	-

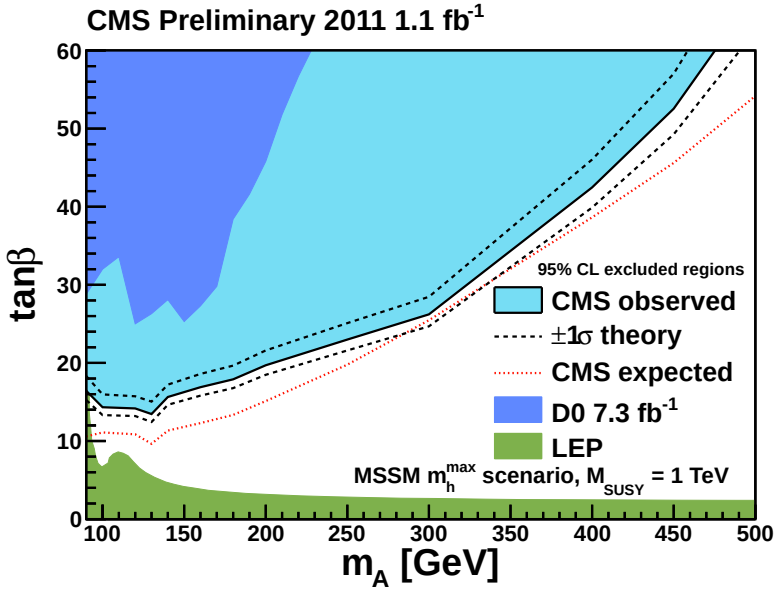

Figure 6: Region in the parameter space of $\tan\beta$ versus m_A excluded at 95% CL in the context of the MSSM $m_h^{\max}$ scenario, with the effect of $\pm 1\sigma$ theoretical uncertainties shown. The other shaded regions show the 95% CL excluded regions from the LEP and Tevatron experiments.

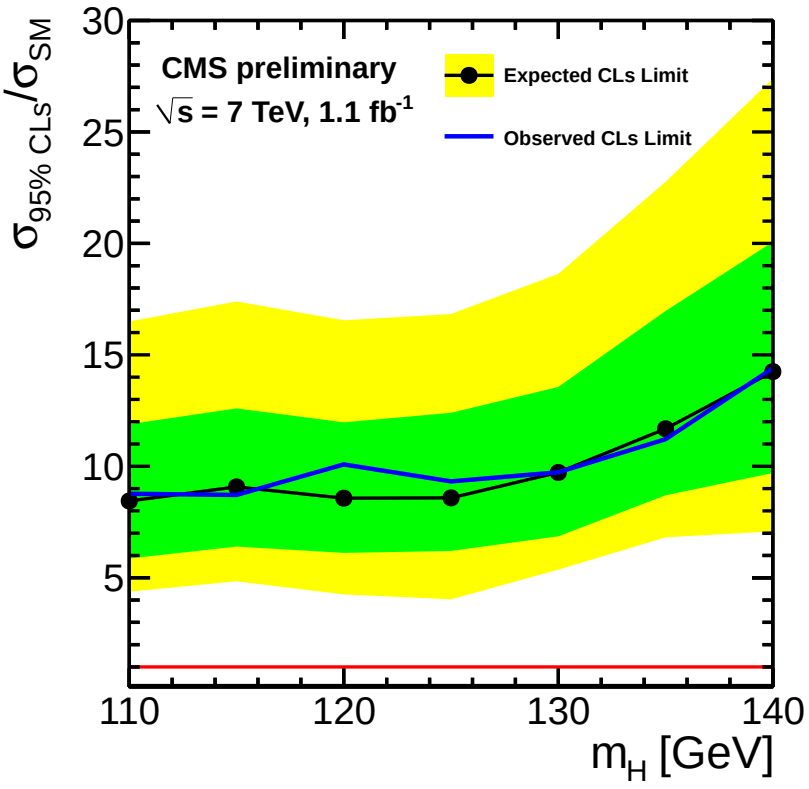

Figure 7: The expected one- and two-standard-deviation ranges and observed 95% CL upper limits on $\sigma_H \cdot B_{\tau\tau}$ normalized to the SM expectation as a function of m_H.

Table 6: Expected range and observed 95% CL upper limits for $\sigma_H \cdot B_{\tau\tau}$ normalized to the SM expectation as functions of m_H, for the SM search.

95% CL Upper Limit						
m_H	Expected $\sigma_H \cdot B_{\tau\tau}$					Observed
(GeV)	-2σ	-1σ	Median	$+1\sigma$	$+2\sigma$	
110	3.0	5.5	7.8	11.0	16.2	8.2
115	2.5	5.9	8.4	12.6	17.9	8.4
120	4.5	5.9	7.5	12.1	15.8	10.0
125	1.0	5.7	8.2	13.0	16.4	9.3
130	3.0	5.6	8.7	13.2	18.0	8.6
135	5.2	7.9	12.1	17.5	21.6	11.6
140	6.5	8.3	13.0	20.1	27.2	13.6

LHC, corresponding to an integrated luminosity of 1.1 fb^{-1}. The tau-pair decay mode in final states with one e or μ plus a hadronic decay of a tau, the eμ and the $\mu\mu$ final state were used, and split into final states with b-tagged jets for the MSSM search and forward jets from VBF for the SM search. In the MSSM case the observed tau-pair mass spectrum reveals no evidence for neutral Higgs boson production, and we determine an upper bound on the product of the Higgs boson cross section and tau-pair branching fraction as a function of m_A. These results, interpreted in the MSSM parameter space of $\tan\beta$ versus m_A, in the m_h^{max} scenario, exclude a previously unexplored region reaching as low as $\tan\beta = 14.2$ at $m_A = 120$ GeV. In the SM case the statistical level is low, and the observed and predicted mass spectra can be incorporated into combined multi-channel searches for the SM Higgs boson. We set an upper limit on $\sigma_H \cdot B_{\tau\tau}$ of 10 times the SM value at $m_H = 120$ GeV.

References

[1] P. W. Higgs, "Broken Symmetries, Massless Particles and Gauge Fields", *Phys. Lett.* **12** (1964) 132. doi:10.1016/0031-9163(64)91136-9.

[2] P. W. Higgs, "Broken Symmetries and the Masses of Gauge Bosons", *Phys. Rev. Lett.* **13** (1964) 508. doi:10.1103/PhysRevLett.13.508.

[3] F. Englert and R. Brout, "Broken Symmetry and the Mass of Gauge Vector Mesons", *Phys. Rev. Lett.* **13** (1964) 321. doi:10.1103/PhysRevLett.13.321.

[4] G. Guralnik, C. Hagen, and T. Kibble, "Global Conservation Laws and Massless Particles", *Phys. Rev. Lett.* **13** (1964) 585. doi:10.1103/PhysRevLett.13.585.

[5] P. W. Higgs, "Spontaneous Symmetry Breakdown without Massless Bosons", *Phys. Rev.* **145** (1966) 1156. doi:10.1103/PhysRev.145.1156.

[6] E. Witten, "Mass Hierarchies in Supersymmetric Theories", *Phys. Lett. B* **105** (1981) 267. doi:10.1016/0370-2693(81)90885-6.

[7] S. P. Martin, "A Supersymmetry Primer", (1997). arXiv:hep-ph/9709356. See also references therein.

[8] CMS Collaboration, "Search for Neutral MSSM Higgs Bosons Decaying to Tau Pairs in pp Collisions at $\sqrt{s} = 7$ TeV", *to appear in Phys. Rev. Lett* (2011).

[9] CDF and D0 Collaboration, "Combined CDF and D0 Upper Limits on MSSM Higgs Boson Production in Tau-Tau Final States with up to 2.2 fb^{-1}", arXiv:1003.3363.

[10] ATLAS Collaboration, "Search for neutral MSSM Higgs Bosons Decaying to $\tau^+\tau^-$ Pairs in Proton-Proton Collisions at $\sqrt{s} = 7$ TeV with the ATLAS Experiment", **ATLAS-CONF-2011-024** (2011).

[11] LEP Higgs Working Group, "Search for Neutral MSSM Higgs Bosons at LEP", *Eur. Phys. J.* **C47** (2006) 547–587. doi:10.1140/epjc/s2006-02569-7.

[12] CMS Collaboration, "The CMS Experiment at the CERN LHC", *JINST* **0803** (2008) S08004. doi:10.1088/1748-0221/3/08/S08004.

[13] CMS Collaboration, "Electron Reconstruction and Identification at $\sqrt{s} = 7$ TeV", *CMS Physics Analysis Summary* **CMS-PAS-EGM-10-004** (2010).

[14] CMS Collaboration, "Performance of muon identification in pp collisions at $\sqrt{s} = 7$ TeV", *CMS Physics Analysis Summary* **CMS-PAS-MUO-10-002** (2010).

[15] CMS Collaboration, "Particle–Flow Event Reconstruction in CMS and Performance for Jets, Taus, and $E_{\mathrm{T}}^{\mathrm{miss}}$", *CMS Physics Analysis Summary* **CMS-PAS-PFT-09-001** (2009).

[16] CMS Collaboration, "Commissioning of the Particle-Flow Reconstruction in Minimum-Bias and Jet Events from pp Collisions at 7 TeV", *CMS Physics Analysis Summary* **CMS-PAS-PFT-10-002** (2010).

[17] CMS Collaboration, "Performance of tau reconstruction algorithms in 2010 data collected with CMS", *CMS Physics Analysis Summary* **CMS-PAS-TAU-11-001** (2011).

[18] CDF Collaboration, "Search for MSSM Higgs Decaying to Tau Pairs", *CDF Public Note* **7161** (2004).

[19] C.C.Almenar, "Search for the neutral MSSM Higgs bosons in the tau tau decay channels at CDF Run II", *PhD Thesis* (2008).

[20] J. Alwall et al., "MadGraph/MadEvent v4: The New Web Generation", *JHEP* **09** (2007) 028, arXiv:0706.2334. doi:10.1088/1126-6708/2007/09/028.

[21] CMS Collaboration, "Measurement of Inclusive W and Z Cross Sections in pp Collisions $\sqrt{s}$=7 TeV", *JHEP* **1101** (2011) 080. doi:10.1007/JHEP01(2011)080.

[22] Z. Wąs et al., "TAUOLA the Library for Tau Lepton Decay", *Nucl. Phys. B, Proc. Suppl.* **98** (2001) 96. doi:10.1016/S0920-5632(01)01200-2.

[23] CMS Collaboration, "Commissioning of b-jet identification with pp collisions at $\sqrt{s} = 7$ TeV", *CMS Physics Analysis Summary* **CMS-PAS-BTV-10-001** (2010).

[24] CMS Collaboration, "Measurement of CMS Luminosity", *CMS Physics Analysis Summary* **EWK-10-004** (2010).

[25] LHC Higgs Cross Section Working Group, S. Dittmaier, C. Mariotti et al., "Handbook of LHC Higgs Cross Sections: Inclusive Observables", arXiv:1101.0593.

[26] CMS Collaboration, "Performance of b-jet identification in CMS", *CMS Physics Analysis Summary* **CMS-PAS-BTV-11-001** (2011).

[27] J. S. Conway, "Nuisance Parameters in Likelihoods for Multisource Spectra", *submitted to Proceedings of PhyStat 2011* (2011) arXiv:1103.0354.

[28] M. S. Carena et al., "Suggestions for Benchmark Scenarios for MSSM Higgs Boson Searches at Hadron Colliders", *Eur. Phys. J.* **C26** (2003) 601–607. doi:10.1140/epjc/s2002-01084-3.

[29] M. S. Carena et al., "MSSM Higgs Boson Searches at the Tevatron and the LHC: Impact of Different Benchmark Scenarios", *Eur. Phys. J.* **C45** (2006) 797–814. doi:10.1140/epjc/s2005-02470-y.

[30] R. V. Harlander and W. B. Kilgore, "Next-to-next-to-leading order Higgs production at hadron colliders", *Phys. Rev. Lett.* **88** (2002) 201801. doi:10.1103/PhysRevLett.88.201801.

[31] R. V. Harlander and W. B. Kilgore, "Production of a pseudo-scalar Higgs boson at hadron colliders at next-to-next-to leading order", *JHEP* **10** (2002) 017. doi:10.1088/1126-6708/2002/10/017.

[32] M. Spira, "HIGLU: A Program for the Calculation of the Total Higgs Production Cross Section at Hadron Colliders via Gluon Fusion including QCD Corrections", arXiv:hep-ph/9510347.

[33] S. Dittmaier, M. Kramer, and M. Spira, "Higgs radiation off bottom quarks at the Tevatron and the LHC", *Phys. Rev.* **D70** (2004) 074010. doi:10.1103/PhysRevD.70.074010.

[34] S. Dawson, C. Jackson, L. Reina et al., "Exclusive Higgs boson production with bottom quarks at hadron colliders", *Phys. Rev.* **D69** (2004) 074027, arXiv:hep-ph/0311067. doi:10.1103/PhysRevD.69.074027.

[35] R. V. Harlander and W. B. Kilgore, "Higgs boson production in bottom quark fusion at next-to- next-to-leading order", *Phys. Rev.* **D68** (2003) 013001. doi:10.1103/PhysRevD.68.013001.

[36] R. Harlander, M. Kramer, and M. Schumacher, "Bottom-quark associated Higgs-boson production: reconciling the four- and five-flavour scheme approach", **CERN-PH-TH/2011-134 - FR-PHENO-2011-009 - TTK-11-17 - WUB/11-04** (2011).

[37] S. Heinemeyer, W. Hollik, and G. Weiglein, "FeynHiggs: a program for the calculation of the masses of the neutral CP-even Higgs bosons in the MSSM", *Comput. Phys. Commun.* **124** (2000) 76–89. doi:10.1016/S0010-4655(99)00364-1.